Abstract

This study investigates the characteristics of rain-on-snow (ROS) events on the summit of Mount Washington, New Hampshire, using data from the daily weather observations taken at the Mount Washington Observatory from 1981 to 2020 to create two different climatologies (1981-2010 and 1991-2020). Several metrics were used to evaluate ROS events, including the frequency and duration of ROS events, the total amount of precipitation during the events, and their impact on snowpack stability and the surrounding watershed. Based on these metrics, several statistically significant ($p < 0.05$) trends were found in the data set, and a case study was then performed to investigate the characteristics of a ROS event that occurred on December 18-19, 2023, which resulted in record flooding across the majority of Northern New England. Notably, a positive increase in ROS events was found for both climatologies, but the highest increase happened in the most recent two climatologies. Furthermore, the decadal trends showed that the most recent decade (2011-2020) shifted the maximum number of ROS events from November to December relative to the other three decades (1981-2010), indicating a shortening winter season and weakening snowpack. Additionally, the December 2023 event case study showed how the snowpack characteristics at the beginning of the winter season can significantly contribute to the flooding associated with ROS events, particularly one that produced an 800-year flood.

1) Introduction

Anthropogenic climate change is affecting many weather and climate extremes across the globe with hot extremes, including heatwaves, becoming more frequent and more intense since the 1950's. At the same time cold extremes have generally become less severe and less frequent (Hans-O 2023). Continued global warming is further projected to intensify the global water cycle and its variability creating very wet or very dry weather and climate cycles. Other projected impacts are increased intensification of tropical storms and the potential for abrupt shifts in regional weather patterns (Hans-O 2023). Climate extremes in the northeast portion of the United States have seen similar trends. Between 1870 and 2005 temperature indices showed a strong warming with an increased frequency of warm weather events and a decrease in cold weather events (Brown et al. 2010) with some arguing that the northeast, specifically New England, is warming faster than many other regions globally (Young and Young 2021). New England is known for its distinctive four season climate and a decline in this will have detrimental effects on the ecology and economy of New England. Signs of a warming climate have already been observed in the form of increased heat waves, decreased snowpack, and more extreme flooding or droughts (Young and Young 2021).

Warming New England winters can impact the type of precipitation across the region as well as the quality of the snowpack. The season that is experiencing the greatest warming across New England is the winter with New Hampshire winter temperatures increasing on average of 2.5 °C on a decadal scale between 1900 and 2020 (Young and Young 2021). A significant consequence of climate warming is the increase of rain on snow (ROS) events (Rennert et al. 2009). Periods of winter warming with near surface temperatures above 0 °C are becoming more frequent (Sobota et al. 2020; Peeters et al. 2019; (Graham et al. 2017)). These events are typically characterized as exceedingly warm weather episodes combined with, sometimes intense, rainfall (Vikhamar-Schuler et al. 2016). These extreme weather events have implications for snowpack, potentially destabilizing alpine snowpack (Mccabe et al. 2007) contributing to avalanches, flooding, as well as impacting the alpine ecosystems with icing events.

Despite Mount Washington being the tallest peak in New England with the summit situated in a sub-Arctic / alpine zone, it has not escaped the effects of regional climate changes. It was found that since 1935 the summit of Mount Washington has warmed an average 0.10 °C per decade with the winter months warming at a greater rate of 0.14 °C per decade (Murray et al. 2021). It is theorized that previous studies done in regards to climate variability on the summit of Mount Washington have not accurately captured trends in regards to the extreme events occurring on summit. Additionally, multiple studies looking at the snowpack on the summit of Mount Washington (Seidel et al. 2009; Murray et al. 2021) state that there has been little noticeable change to the summit winter snowpack. These studies however fail to look into the impacts of warming events and ROS that detrimentally impact winter snow cover. Additionally these studies fail to observe the overall increase or decrease in precipitation and type of precipitation on the top of New England's highest peak.

The scope of this study aims to accurately establish and quantify climate trends related to extreme weather events occurring on the summit of Mount Washington for the period of October 1980 through May of 2020. This will be done by taking the 10 and 30 year averages looking at the overall temperature, and precipitation changes as well as selecting an outlier from recent years relative to the 30 year averages to look the impacts of ROS events at the summit of Mount Washington. This extreme event will be selected as values that trend far from the period average and include events that have broken daily, monthly, yearly, or all time records

This study will further investigate the changing seasonality around the winter on Mount Washington to determine if winters are warming and if this is impacting the summit snowpack as well as shifting the seasonality. By isolating winter precipitation events when there is a definable snowpack on the ground, it will be possible to see if there has been an increase in ROS events on the summit. This will help to determine if the winter precipitation on Mount Washington has been increasing while warmer temperatures allow rainfall increasing icing events and winter water runoff into neighboring ravines and gullies. Determining how winter is impacting Mount Washington will increase the understanding of how climate change is impacting the region in addition to adding to the knowledge of how the fragile high alpine zones will be impacted globally by a continued changing climate.

2) Lit Review

ROS (Rain-on-Snow) has become an increasingly prevalent research topic globally, with many studies focusing on similar variables during their analyses. The selection of specific criteria often

depends on the goals of each study, and Figure #1 shows the various thresholds used for each variable across different ROS studies..

Literature	Rainfall threshold/liquid precipitation (mm)	Snow cover threshold	Data	Research area
Liston and Hiemstra (2011)	≥3	SWE ≥5 mm	MERRA	North of 55°N
Cohen et al. (2015)	≥10	SCF ≥ 50%	MERRA	North of 50°N
Würzer et al. (2016)	≥20	SD≥25 cm	IMIS[a] network stations records	Switzerland
Trubilowicz and Moore (2017)	≥5	SWE ≥10 mm	Automated snow pillow sites records	South coastal British Columbia, Canada
Musselman et al. (2018)	≥10	SWE ≥10 mm	WRF[b] simulations	Western North America
Li et al. (2019)	≥3	SWE ≥10 mm	VIC[c] simulations	Conterminous United States
Vickers et al. (2022)	≥5	SWE ≥3 mm	seNorge[d]	Norway
Personal definition	≥0.5 (Dou et al., 2021)	SCF=100%		

FIGURE #1: Table of the thresholds used for each variable in various ROS studies

Most previous ROS studies have relied on a mix of data sources such as meteorological station records, satellite remote sensing datasets, and atmospheric reanalysis products. Meteorological station records are particularly effective for local-scale ROS evaluations due to their precision (Vickers et al. 2022). For example, Putkonen and Roe (2003) used in-situ station observations to assess ROS impacts on soil temperature, comparing these observations with large-scale reanalysis to verify the accuracy of model outputs. However, the limitation of station data lies in its inability to provide a broader scale estimation of ROS events, making the choice of data dependent on the study's specific objectives (Tao et al. 2023).

Despite a variety of ROS definitions, they generally fall into two categories. The first category defines thresholds based on the smallest measurable amounts to include all possible ROS events within a given timeframe. The second category, exemplified by Freudiger et al. (2014), focuses on the minimum thresholds necessary for a ROS event to cause flooding. This definition was informed by the re-analysis of a significant 2011 ROS event and was chosen due to the lack of sufficient in-situ weather observations over the larger study area.

Freudiger et al. (2014) also addressed the challenge of selecting an appropriate time scale for evaluating ROS events, choosing a range from November 1st to May 31st to avoid splitting winter seasons between years and to minimize bias from snowless summer months. By grouping consecutive days meeting ROS

criteria into single events, they could better assess the impacts on stream discharge, often delayed relative to the start of the ROS event.

The study also explored trends in ROS events, such as frequency and magnitude. They found that ROS events were more common in early winter (November–February) than in late winter (March–May). However, the frequency of ROS events over time yielded mixed results depending on the location. When examining magnitude, defined as the equivalent precipitation depth (Peq) of a ROS event, they identified significant decreasing trends during the late winter season using a non-parametric Mann-Kendall test at a 5% significance level (Mann 1945).

Analyzing trends in ROS events can be challenging due to the irregular occurrence of ROS days. Pall et al. (2019) addressed this by applying a Theil-Sen estimator (Sen 1968; Theil 1950) alongside a Mann-Kendall test, both non-parametric methods suitable for the often non-normally distributed hydrometeorological data (Yue and Pilon 2004).

Data collection methods vary, each with its benefits and limitations. While meteorological station records, satellite datasets, and atmospheric reanalysis are common sources, the discrepancies between them can complicate model evaluations, especially for future ROS event predictions (Vickers et al. 2022). Typically, ROS is detected in observational and simulation data by defining thresholds for temperature, precipitation, and snow cover. However, the finer spatial scale of observations compared to model grid data presents challenges in direct comparisons. Vickers et al. (2022) proposed using ground-based observations as the "gold standard" for comparison and emphasized the importance of considering observation uncertainties to avoid incorrect conclusions about model performance.

ROS events are known for causing significant flooding, as seen in the 2013 South Saskatchewan and Elk River Basin flood in Canada, which was the costliest natural disaster in the country's history at the time (Pomeroy et al. 2016). Another example is the 2017 ROS event in California, which severely damaged the Oroville Dam, leading to the evacuation of nearly 200,000 people (Vahedifard et al. 2017). The high flood potential of ROS events stems from the combination of rainfall and snowmelt, with the timing of water release from snowpack playing a critical role (Kattelmann 1996). The main factors influencing ROS floods include the extent of snow cover, freeze/thaw elevations, snowpack SWE, and the intensity and duration of liquid precipitation.

Forecasting ROS floods is challenging due to the complex interactions within snowpacks. For example, a snowpack's composition can significantly impact runoff generation. Ice layers within the snowpack can double its water-holding capacity, while preconditioning may enhance flow rates (Singh et al. 1997). The spatial variability of snowpacks, combined with limited SWE data, complicates the prediction of ROS events and their runoff responses, which are crucial for flood mitigation.

3) Data

Primary meteorological observations used in this case study were collected at the Mount Washington Observatory (MWO), located at the summit of Mount Washington in the Presidential Range

within the White Mountain National Forest (Fig. 2). The National Geologic Survey places the summit elevation at 6286 ft with treeline typical ranging between 1100m and 1500m in elevation (Kimball and Weihrauch 2000). MWO observers have been working at the summit year-round since 1932 and currently operate as a National Weather Service "cooperative station" by submitting hourly and six hourly synoptic weather observations. Over the years, MWO has used several buildings for its operations, but the station moved to its current location, the Sherman Adams building, in August of 1980. The station's current location on the summit is 91m farther north and 6m higher in altitude than the previous station locations (Seidel et al. 2007).

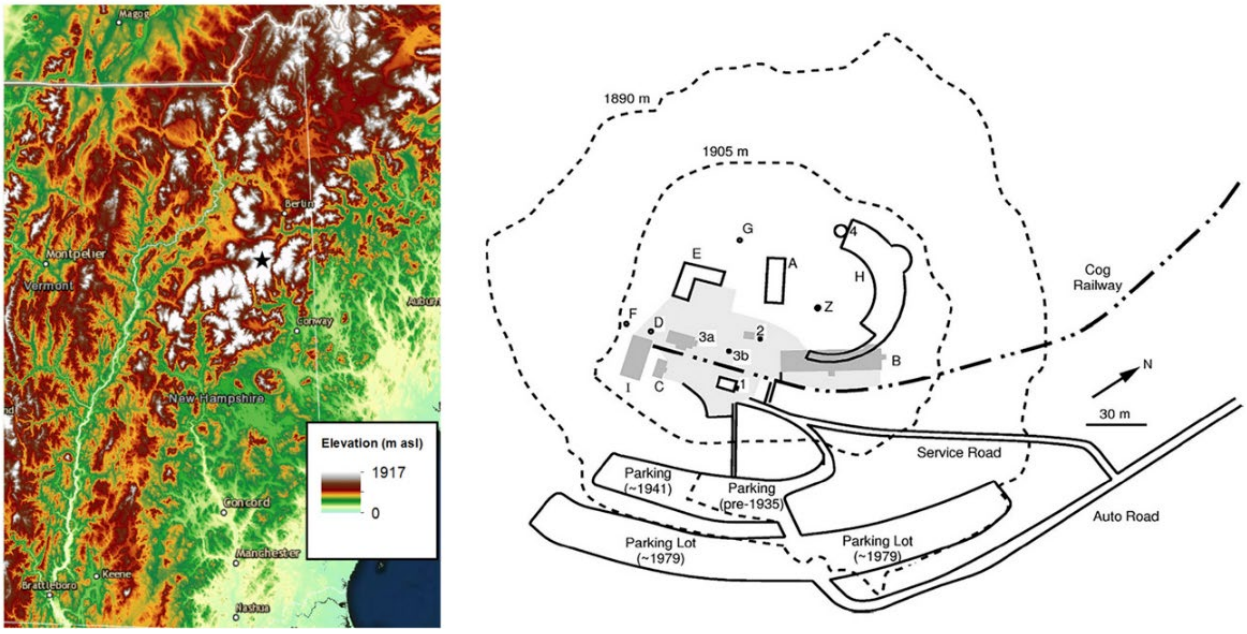

FIG. 2. (left) Location of Mount Washington (black star) in northern New Hampshire (digital elevation model was provided through the courtesy of The Nature Conservancy and The Wildlife Conservation Society; https://www.sciencebase.gov/arcgis/rest/services/Catalog/5395cfaae4b0b4b172cbe6b3/MapServer/). (right) The locations of large structures (letters) and the location chronology of the maximum– minimum thermometer shelters (numbers) that are adjacent to where hourly sling psychrometer observations were taken. Structures still in existence are outlined in black. Locations of demolished structures are in dark gray. The present-day area of graded dirt and gravel is in light gray. The shelter location chronology is as follows: 1 5 beginning of record to 23 Jun 1936, outside the northwest side of the Stage Office entrance; 2523 Jun 1936–21 Oct 1937, outside the northwest wall of the vestibule of Camden Cottage (the black dot next to 2 is the current location of the precipitation can); 3a 5 21 Oct 1937–1 Aug 1980 (except for periods noted for 3b), northwest wall of vestibule of ‘‘new’’ observatory building; 3b 5 June–October for the years 1937–40 and 22 Jul–21 Oct 1941, northeast face of a 34-ft-tall observatory tower; 451 Aug 1980–present, outside observation deck entrance on the northeast side of the observatory tower entrance to the Sherman Adams Summit Building. The structures are as follows: A 5 Tip Top House (1853–present), B 5 Third Summit House (1915–80), C 5 Alford power (generator) house (1937–2003), D 5 Alford antenna tower (1937–present), E 5 Yankee Building (1941–present), F 5 FM radio antenna tower (1952–present),G5FM radio antenna tower (1988–present),H5Sherman Adams building (1980–present), and I5 WMTWtransmitter building (1954–2003); Z 5 the geographical summit at 1917 m. Dashed lines are height contours for 1890m (6200 ft) and 1905m (6250 ft). From 1980 to present, snow depth has been estimated across the graded dirt and gravel area between the southern end of the Sherman Adams Summit Building and the precipitation can. This map is adapted from Grant et al. (2005) and Kelsey and Cinquino 2021.

B) Precipitation type, amount, and temperature datasets

A sling psychrometer has been used by weather observers since January 1st, 1935, to take dry-bulb and wet-bulb temperature measurements on the summit. The full details of the process behind taking measurements with a sling psychrometer can be seen in Seidel et al. (2007). All values in this study were obtained from the MWO digital database, which contains all hourly and six hourly temperature values. Despite automated measurements being taken at the summit in recent decades, they are often too error-prone to be reliable. The cold season (October – May) tends to be when the automated instruments are most unreliable because icing conditions are most prevalent, and wind speeds often exceed 67 mph (Kelsey and Cinquino 2021). Therefore, a sling psychrometer is more

accurate since it is kept inside between hourly weather observations and can avoid being encased in a ball of ice

For this study, hourly and six hourly temperatures, hourly precipitation types, six hourly precipitation totals, and daily snow depth data were obtained for the winter years (October – May) from 1981 to 2020. The data set was investigated for any missing data, but little to no missing data points were found. Therefore, missing data had a negligible impact on the results of our study. However, several erroneous data points were found in the online database but not in the physical records used to create the digital database. Therefore, the discrepancy is likely because of human error when the physical records were transcribed to our digital database.

Additionally, snow depth and precipitation measurements were subject to unique errors due to how they were obtained. Specifically, snow-depth observations are subjective and prone to error in their accuracy since observers visually estimate them, but previous studies have failed to quantify the magnitude of the error associated with them. Snow-depth observations were only used in our case study to quantify the snowpack loss, not necessarily depth, during the ROS event since the change in snow depth between observations tends to be significantly less error-prone (Kelsey and Cinquino 2021).

For the rest of the study, hourly precipitation types and six hourly precipitation totals were used to quantify the effect of ROS events on the summit due to their higher accuracy. Weather observers go outside every hour to physically observer the precipitation type using a primitive snowboard to catch the precipitation and then closely observe it before it melts. However, six hourly precipitation totals tended to have a slightly larger error associated with them than the hourly precipitation types did due to the effects of blowing snow. As previously mentioned, winds commonly exceed 67 mph on the summit during the cold season, so they can lead to an undercatchment if high winds cause the falling snow to blow sideways over the can instead of falling straight into it. Moreover, high winds can also lead to overcatchment when they cause blowing snow to fall in the can and add to the snow that has already fallen.

C) Stream Area:

The Mount Washington Summit marks an intersection between three watersheds, Headwaters Ammonoosuc River, Peabody River-Androscoggin River, and Ellis River. Given that there is currently no stream gauge located in the Ellis River watershed, the Headwaters Saco River watershed is also included as it drains directly from the summit, though its border falls short of the true summit. These three watersheds are each contained within distinct hydrologic units; Headwaters Ammonoosuc in the Upper Connecticut unit, Peabody-Androscoggin in the Lower Androscoggin unit, and Headwaters Saco in the Saco unit.

Two stream gauges are located along the Saco river, in the Saco hydrologic unit, one in Bartlett and one in Conway NH. Located in the Headwaters Saco watershed, the Bartlett gauge has an elevation of 660ft NAVD88, 5626ft lower than the summit. Mean basin slope was calculated to be 30 degrees and drainage area to be 91sq mi. Summit runoff to this gauge occurs primarily through the Dry River, on the south facing side of Mount Washington. Located further to the south, in the Conway Lake-Saco River watershed, the Conway gauge has an elevation of 418ft NAVD88, placing it 5868ft below the summit, with a mean basin slope of 23 degrees. This gauge has a much larger drainage area, of 385sq mi. Despite

its distance, the Conway gauge also drains from the Mount Washington summit, though its summit runoff comes by way of the Ellis River and Rocky Branch, in addition to the Dry River.

The Ammonoosuc gauge, situated in Bethlehem, NH, receives most of its summit runoff from the Ammonoosuc River, which flows along western aspects of the mountain. It also receives water from Clay and Jefferson Brooks via the Ammonoosuc and Burt Ravines. This gauge is located at an elevation of 794ft NAVD88, 5492ft below the summit, with a mean basin slope of 22 degrees. This is the smallest drainage examined, with a drainage area of 87.6sq mi.

The Peabody-Androscoggin gauge, located in Gorham NH, receives most of its summit runoff from the West Branch Peabody River through the Great Gulf area, giving it a mostly northern aspect. Unfortunately, headwater storage and various flood mitigation strategies employed along the Androscoggin have the potential to artificially increase discharge values; as such, the gauge and its data has been removed from this study.

Mount Washington can be separated into four distinct areas of surficial deposits. The summit cone, where precipitation data is recorded, consists of upper slope diamicts. These are angular, heavily weathered cobble to boulder sized clasts of alpine metamorphic lithologies, sitting atop bedrock. While this setup is conducive to producing runoff, the holding capacity of this alpine region is quite low. Most precipitation falling on the summit will therefore runoff to lower elevations (Dethier et al. 2022). The ravines, existing in the subalpine region below the summit, are composed of two surficial units, both colluvial debris but distinguished by their location either on or below the unstable and rockfall prone slopes of the ravines. This debris consists of cobble to boulder sized clasts, matrix dominated diamicts and talus. Middle elevations outside of the ravines are composed of lower slope diamicts of variable size and weathering, likely originating from the higher elevations. This is the highest elevation on the mountain with significant areas of silt and clay, treeline is also located in the middle elevations at roughly 4500ft (Leak and Graber 1974). Water infiltration in this region is limited by the small amounts of clay and silt overlying bedrock (Heath et al. 2004). Lower elevations, below ravine level, consist of till, with variable clasts and silt, sand, and clay. These deposits are generally less than 20ft deep but can reach up to 100ft beneath hillocks and moraine features (Fowler 2010).

4) Methods

A) Combining Data Sets

Two 30-year climatologies (1981-2010 and 1991-2020) of daily Rain on Snow (ROS) events will be created to analyze long-term trends. Present weather data, snowfall, snow depth, precipitation, and temperature will be compiled by corresponding dates. Hourly observations within six hours of a synoptic observation are matched to form a unified dataset. The final dataset includes daily maximum/minimum snow depth, total liquid precipitation, snowfall, and present weather types.

B) Our Criteria for identifying a daily ROS event

To identify ROS days, the dataset is filtered based on specific criteria. A minimum snow depth of one inch at the summit ensures rain primarily falls on snow, not the ground. The threshold for measurable rainfall is set at 0.01 inches of liquid precipitation. Precipitation types classified as liquid include rain, rain showers, and drizzle. Frozen precipitation such as hail, snow, or ice crystals is excluded.

The 1981-2010 and 1991-2020 climatologies are created by excluding events not meeting these criteria, with careful handling of liquid/freezing precipitation types based on prior studies.

C) Analyzing the ROS datasets

After the final ROS data sets for both climatologies are created, they will be analyzed to determine long-term trends, seasonality of ROS days, and their effects on the ecosystem and surrounding communities. To evaluate changes from 1981 to 2020, trends will be assessed using the Theil-Sen estimator and Mann-Kendall tests for each climatology (Theil 1950; Sen 1968; Mann 1945).

The dates must be converted from "calendar year" to "winter year" (October to May, designated by the year in which it ends) to avoid splitting winter seasons and eliminating months with little ROS activity. ROS days will also be converted to ROS events, defined as one or more consecutive days meeting the criteria for ROS. Data will include maximum/minimum snow depths, total precipitation, snowfall, event duration, and reported weather types.

Once converted, the average number of ROS days per month will be calculated for each climatology, and seasonality trends can be plotted. Comparisons between recent and past trends will be visualized with line charts and tables. The long-term change of ROS days will be evaluated with the Theil-Sen estimator to determine the trend slope, while non-parametric Mann-Kendall tests will assess the statistical significance of changes at the 5% level.

D) Case Study

The December 2023 ROS event will be characterized using a combination of meteorological, snowpack, and hydrologic data. Initially, the synoptic evolution of this event will be analyzed using historic surface analysis charts, created from local sounding and observational data, from the National Weather Service. Localized development of this event will be analyzed primarily using Mount Washington Observatory archival data. Hourly present weather codes will be obtained from the MWOBS's B-16 archives. Snowfall amounts, snow depth, and liquid precipitation totals, collected every six hours by summit observers, will be obtained from MWOBS's archive of synoptic weather reports. Mount Washington summit data will be supplemented with weather data from the North Conway NCON3 weather station, and observations from the Hermit Lake snow plot, located at the base of Tuckerman Ravine on Mount Washington. MWOBS summit data will be used as a primary data source, with NCON3 and Hermit Lake data used to inform event development at elevations below the summit.

Hermit Lake snow plot observations, in conjunction with observations submitted by the USFS Mount Washington Avalanche Center, will be used to characterize snowpack development in the month preceding this event. MWOBS B-16 hourly weather data and 6 hourly synoptic weather data will be used to confirm MWAC observations. These data are limited to locations above 3,000 ft, so

Community Snow Observations will be used for an approximation of lower elevation snowpack in Carroll NH, located adjacent to the western side of Mount Washington.

Three USGS stream gauges are located in watersheds directly adjacent to the summit. The Ammonoosuc river gauge, in Bethlehem NH, the Peabody River gauge, a tributary of the Androscoggin River, in Gorham NH, and the Saco River gauge, in Bartlett NH. Data from the Peabody gauge will be omitted since head water storage and flood mitigation measures occurring along this river have the potential to create artificially inflated stream flow values. Both daily stream discharge and gauge height values will be used for the two remaining gauges; discharge as an indicator of conditions along the entire river, and gauge height as an indicator of local flooding conditions. These data will be used to determine duration, onset, and intensity of event runoff. Another gauge, further downstream on the Saco River, located in Conway NH, will be used to supplement historic discharge data, with a daily discharge record dating back to 1903. While this gauge is not located in an immediately summit adjacent basin, it is fed directly by flow from the higher summits and has the longest record of any of the available gauges. A Pearson 3 function will be run over the Conway and Bethlehem discharge data sets to determine a recurrence interval for the December 2023 flooding event. Additionally, daily discharge values for this event from the gauges will be directly compared to daily discharge values from previous major hydro-meteorological events in the region.

5) Results

A) Bulk stats of ROS Days

Table #1: Total amount of ROS days for each month defined as a winter year

Month	1981-2010 Total ROS Days	1991-2020 Total ROS Days
October	69	92
November	137	135
December	121	172
January	98	118
February	91	90
March	148	153
April	211	234
May	116	133

Table #2: Total amount of ROS days for each winter year from 1981-2020

Winter Year	Total ROS Days	Winter Year	Total ROS Days
1981	34	2001	20
1982	24	2002	38
1983	34	2003	30
1984	45	2004	33
1985	20	2005	46
1986	26	2006	45
1987	18	2007	43

1988	28	2008	44
1989	29	2009	42
1990	28	2010	36
1991	32	2011	50
1992	33	2012	33
1993	26	2013	37
1994	33	2014	45
1995	30	2015	38
1996	39	2016	48
1997	49	2017	48
1998	20	2018	36
1999	31	2019	44
2000	35	2020	43

ROS days for each winter year from 1981 to 2010 and 1991 to 2020 were calculated, analyzed, and recorded in table #1 and #2. Overall, the total number of ROS days that occurred in the 1981-2010 climatology was slightly less than in the 1991-2020 climatology, with 1016 ROS days and 1190 ROS days, respectively. That averages out to 34 ROS days per year for 1981-2010 and 40 ROS days for the 1991-2020 climatology. However, only about 2% of those ROS days occurred during the warmer months of June, July, August, and September for both climatologies. Furthermore, the month that experienced the most amount of ROS days for both climatologies was April with an average of 7-8 ROS days per month, but there was also a secondary local maximum in ROS days during November for 1981-2010, with an average of around five days per month. There is also a secondary maximum for the 1991-2020 climatology that occurs in December, with an average of around six days per month.

B) Long term trends of ROS observations from 1981-2020

An attempt was made to evaluate ROS observations as opposed to ROS days over the entire range of years from 1981-2020, but the results tended to be messier than when ROS days were analyzed for the two climatologies independently. Out of all the graphs produced and statistical tests completed, ROS observations for 1981-2020 had the lowest statistical significance. It failed the Mann-Kendall test at the 5% significance level with a value of around 14%. Furthermore, the Theil-Sen slope produced in Figure #3 had a slope value of 0.00 and a coefficient of determination of -0.03, so it is also a statistically insignificant result. It was the least significant result of any graph produced during the study. All ROS observational data for 1981-2020 can be seen in table #3

Table #3: Total amount of ROS observations for each winter year from 1981-2020

Winter Year	Total ROS Days	Winter Year	Total ROS Days
1981	37	2001	22
1982	23	2002	55
1983	75	2003	36
1984	54	2004	40
1985	18	2005	62

1986	43	2006	54
1987	31	2007	50
1988	34	2008	56
1989	16	2009	39
1990	46	2010	58
1991	47	2011	45
1992	32	2012	26
1993	25	2013	45
1994	37	2014	54
1995	27	2015	31
1996	68	2016	63
1997	37	2017	43
1998	39	2018	63
1999	39	2019	41
2000	45	2020	52

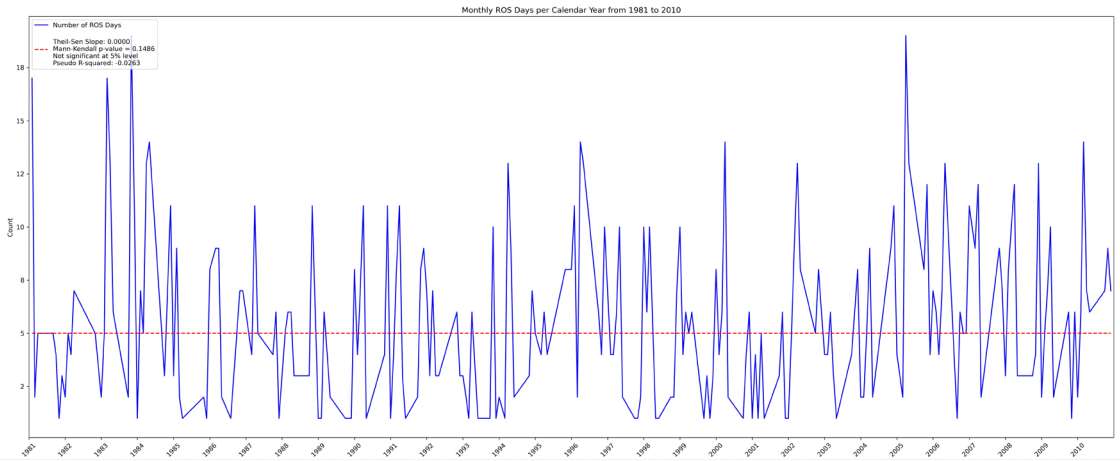

Figure #3: ROS observations per Month from 1981 to 2020. The red line is the calculated Theil-Sen slope and the blue line is the number of ROS events per month.

C) Long term trends of each climatology

After the ROS observations were converted to ROS days and calendar years to winter years, a more statistically significant result was produced for both climatologies. They both passed the Mann-Kendall test at a 5% significance level. The 1991-2020 climatology depicted in Figure #4 had the most significant result, passing the Mann-Kendall test at a 5% and 1% significance level with a value of 0.4%. It also the greatest coefficient of determination produced by the Theil-Sen slope with a value of 0.29. In comparison, the 1981-2010 climatology depicted in Figure #4 was also statistically significant as it passed the Mann-Kendall test at a 5% and 1% significance level with a value of 0.8%. Furthermore, it also had the second-highest coefficient of determination produced by the Theil-Sen slope with a value of 0.21.

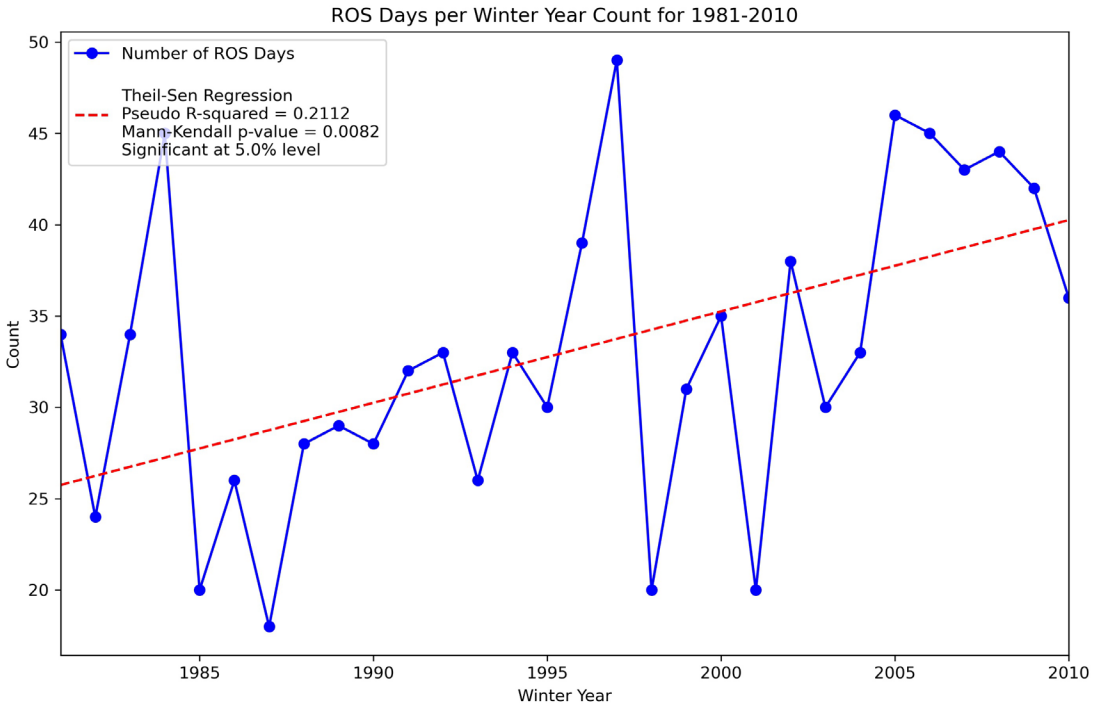

Figure #4: Total ROS days per winter year from 1981 to 2010. The red line is the calculated Theil-Sen slope and the blue line is the number of ROS events per year.

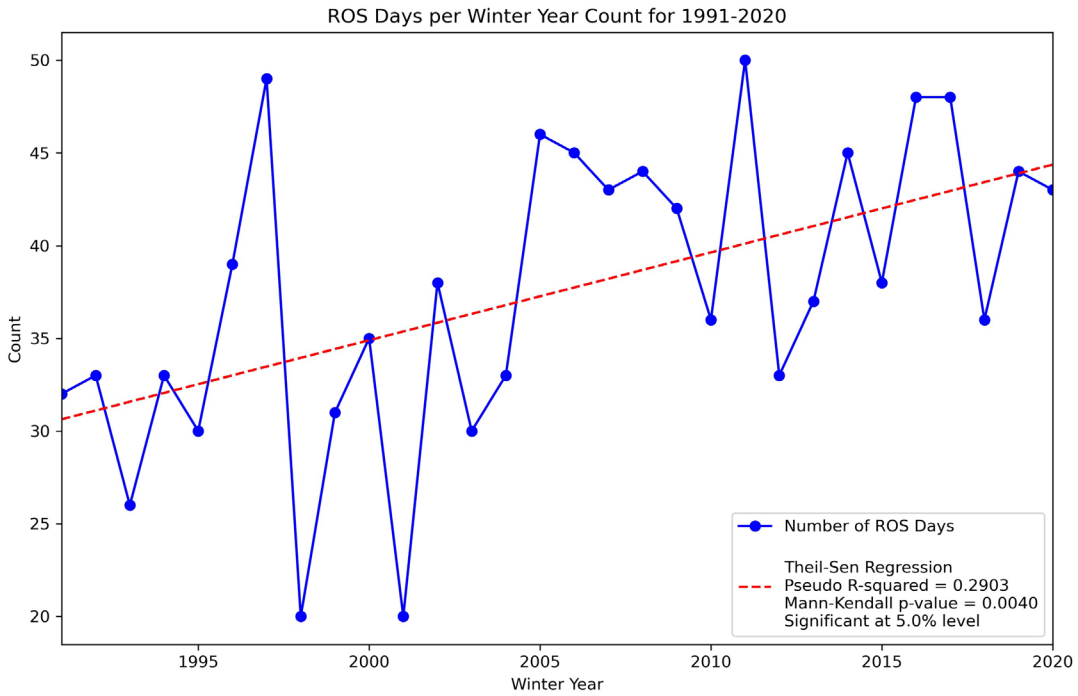

Figure #5: Total ROS days per winter year from 1981 to 2010. The red line is the calculated Theil-Sen slope and the blue line is the number of ROS events per year.

D) ROS Seasonality

Converting ROS observations to ROS days and calendar years to winter years also enabled an evaluation of the seasonality of ROS days. Statistically speaking, there was a 17% increase in the total amount of ROS days from 1981-2010 to 1991-2020, but that wasn't the most significant increase that was observed across the two climatologies. As seen in Figure #5, the greatest average increase occurred during December, with 46% more ROS days occurring between 1991 and 2020 compared to 1981 and 2010. The subsequent most significant increase was observed in January, with 35% more ROS days occurring between 1991 and 2020 compared to 1981 and 2010. The statistical increases between the two climatology's for each month are depicted in table #4.

Table #4: The average amount of ROS days for each month in a winter year

Month	1981-2010 Total ROS Days	1991-2020 Total ROS Days
October	2.3	3.1
November	4.6	4.5
December	4	5.7
January	3.3	3.9
February	3	3
March	4.9	5.1
April	7	7.8
May	3.9	4.4

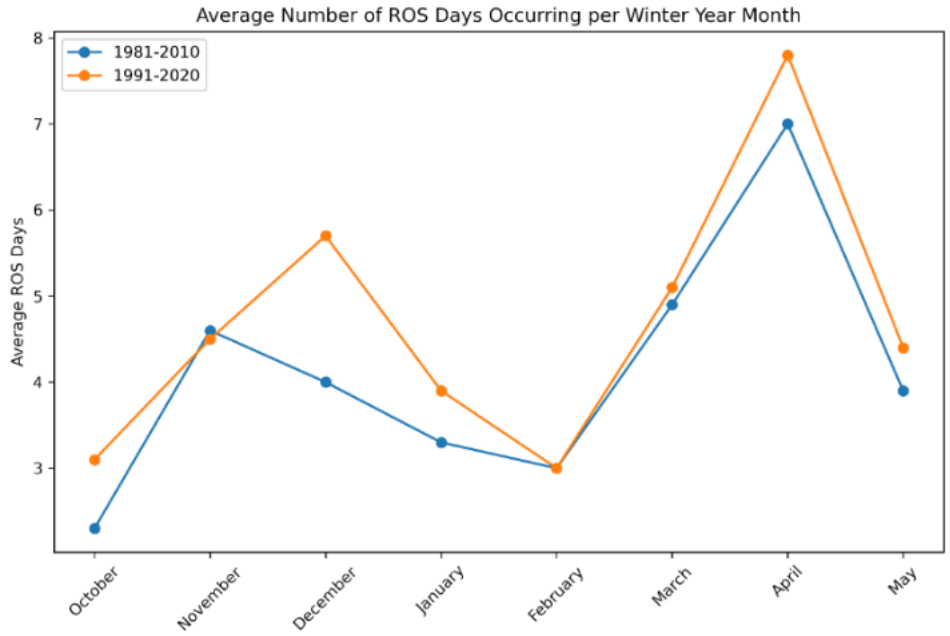

Figure #6: Average amount of ROS days per winter year from 1981 to 2010. The red line is the calculated Theil-Sen slope and the blue line is the number of ROS events per year.

E) Decadal trends of each climatology

A more in-depth analysis was also created to determine the seasonality of ROS events further. The most significant result is the general trends found in the earlier decades (1981-2010) compared to the most recent decade (2011-2020). The total number of ROS days per month depicted in Fig. #4 initially tended to peak in November from 1981 to 2010. However, from 2011 to 2020, November

received the second lowest amount of ROS days per month, with a total of only 34. 2011-2020 is also different from the other decades since the initial peak in ROS days occurred in December, with 94 in total, then decreased in the following few months. In contrast, we experienced declining ROS days in December rather than a local maximum in the other three decades.

The second peak in the total ROS days, and the most prevalent, occurred in the late spring for all decades, with values ranging from 59 (1991-2000) to 94 (2011-2020). Specifically, April is the month that saw the highest amount of ROS days for each decade. The most significant trend during April, except for 1991-2000, was that each decade had higher ROS days than the previous one. In contrast, this second peak in ROS days didn't shift to a different month like the initial peak did when it moved from November in the earlier decades to December for the most recent one.

Furthermore, each decade tended to have similar trends in total ROS days from February through May. February often had one of the lowest ROS days recorded out of all months for each decade used in this study, and the total number of ROS days ranged from 34 in 1981-1990 to 2001-2010. Hence, February had the most minor variability among total ROS days compared to other months. From February onwards, the trends for all decades match up the best as they all have a similarly positive slope and a peak in April.

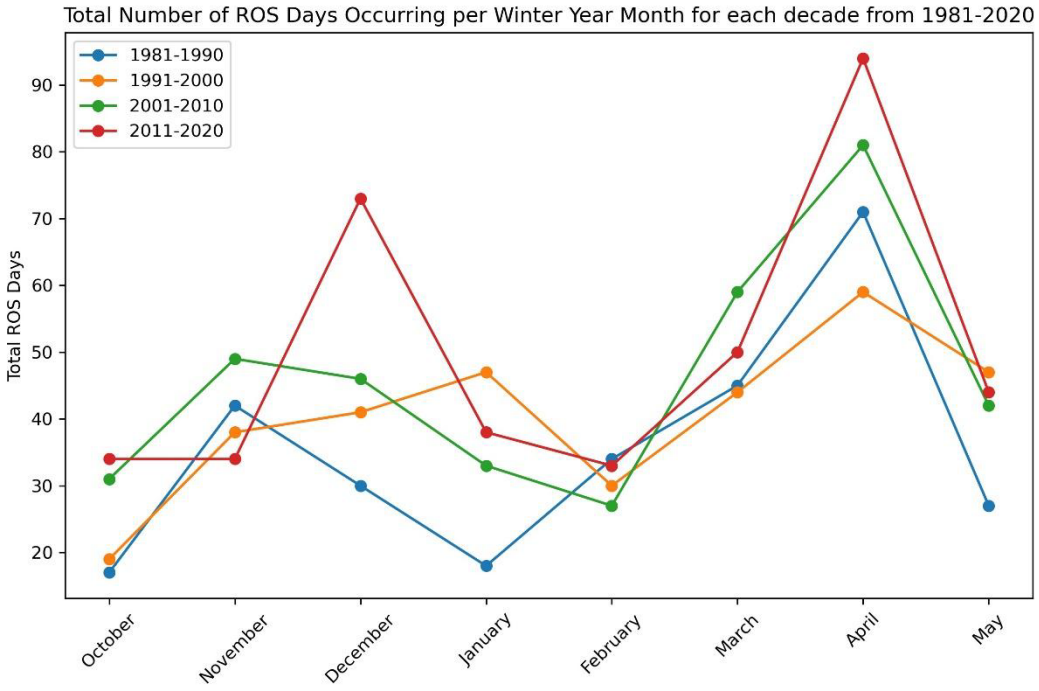

Figure #7: Total amount of ROS days per winter year for each decade from 1981 to 2010. The red line is 2011-2020, green line is 2001-2010, orange line is 1991-2000, and the blue line is 1981-1990.

F) ROS Events/Duration

A closer look into ROS's characteristics at the summit revealed several differences between the climatologies. As seen in table #5 the average duration of a ROS event was the same between

climatologies, with an average of 1.7 days, but that was one of the only similarities between them. The only other similarity is the average total snowfall of 3” for both climatologies.

For the 1991-2020 climatology, the average maximum snow depth during a ROS event was 7.6”, but the average maximum snow depth for the 1981-2010 climatology was slightly lower at 6.3”. Similarly, the 1991-2020 climatology had the highest average minimum snow depth at 6.5” as compared to 1981-2010’s average minimum snow depth of 5.5”. Furthermore, there was also a difference in the average total liquid precip between the two climatologies, but the 1991-2020 climatology had a lower average at 0.99” as compared to the 1981-2010 climatologies average of 1.13”.

Table #5: Statistics averages for all ROS events during the 1991-2020 and 1981-2010 climotologies

Years	Avg. Duration (days)	Avg. Max Snow Depth (in)	Avg. Min Snow Depth (in)	Avg. Total Snow Fall (in)	Avg Total Precipitation (in)
1991-2020	1.7	7.6	6.5	3	0.99
1981-2010	1.7	6.3	5.5	3	1.13

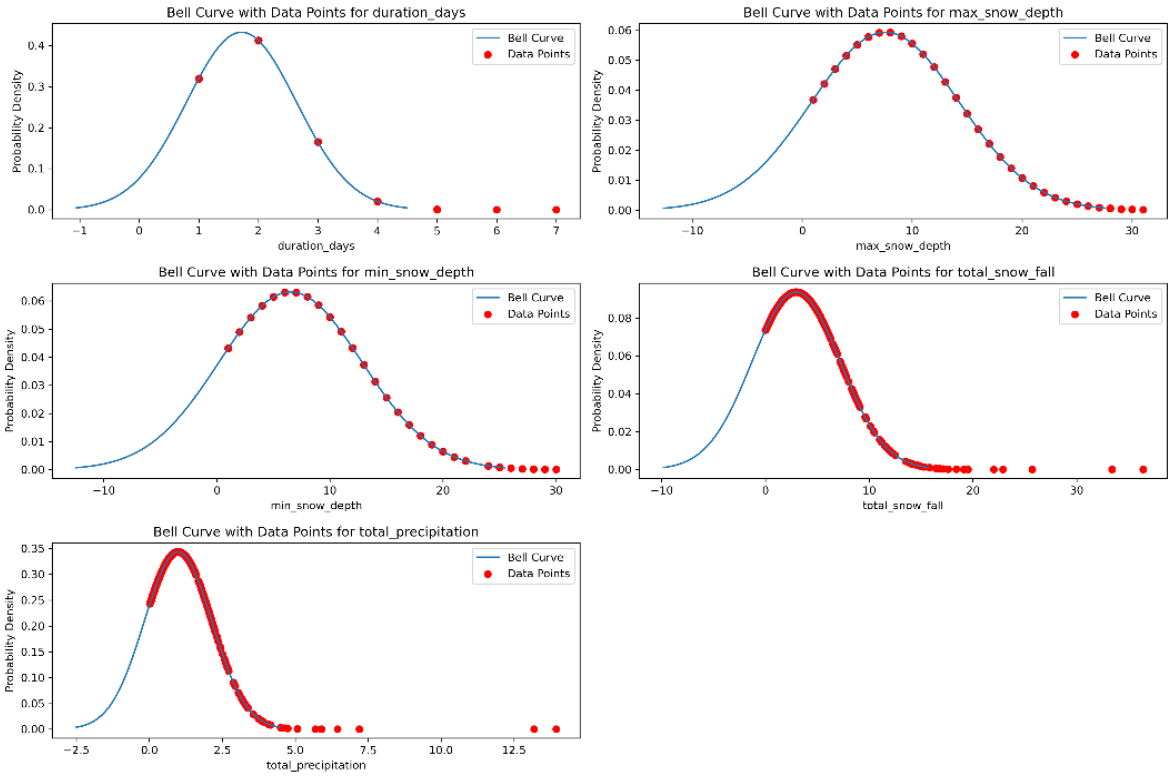

Figure #8: Bell curves of the 1991-2020 ROS Events

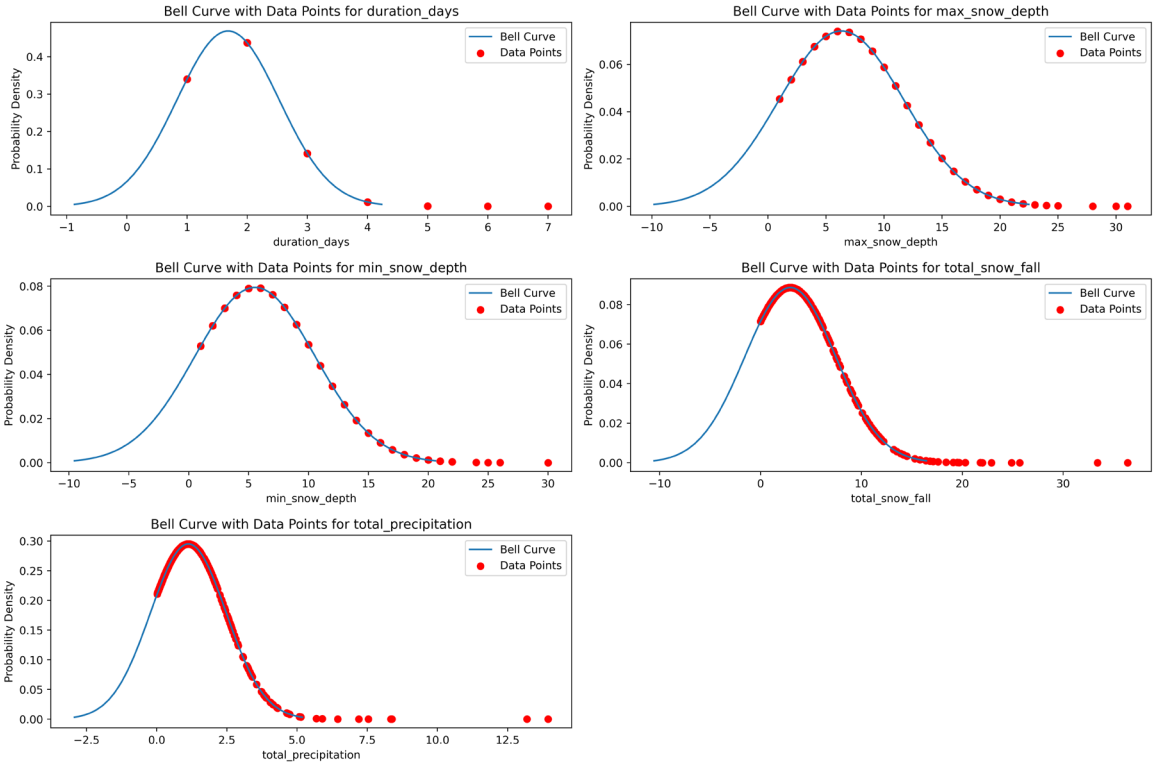

Figure #9: Bell curves of the 1981-2010 ROS Events

G) Case Study

Weather Conditions/Meteorologic Setup:

The weather in the three days preceding the December 2023 ROS event was characterized by generally clear conditions. No precipitation fell at the summit between the 2am observation on Dec 14th and the 4pm observation on December 17th. No precipitation was recorded at the NCON3 station for December 14th through the 17th.

The December ROS event began in the late afternoon of December 17th 2023. The 4pm EST summit observation reported freezing drizzle, becoming a combination of freezing rain/drizzle, ice pellets, and rain, which continued until the 1am EST observation on December 18th. At this observation, summit temperatures rose to 35ºF and precipitation transitioned to rain, which continued for the next 18 hours before becoming a combination of rain and freezing rain at 7pm on December 18th. Precipitation ended completely by the 10pm EST observation that same day. From December 17th to 18th, across 31 hours, this system dropped a total of 4.1 inches of precipitation at the Mount Washington summit. The lower elevation NCON3 station recorded 3.71 inches of precipitation from the same event.

A strengthening low-pressure system moving north along the eastern seaboard resulted in increasing temperatures and precipitation throughout the region. The elongated shape of this low resulted in an extended wind field over the ocean, contributing significant moisture to the system and driving up precipitation totals. By 11am EST on December 18th, the low was centered over New England, with a pressure of 982mb, a 16mb drop from 24 hours prior. Rainfall peaked in intensity at the summit

around 1pm EST on December 18th, with lighter rainfall continuing for hours afterward. The passage of repeated warm fronts spinning off this low drove temperatures up to a new daily record high of 41ºF at the Mount Washington summit before decreasing back below freezing by 6pm EST on December 18th. Primarily clear conditions dominated the week following this event, with only trace precipitation recorded.

Snowpack Composition:

From December 17th to 19th elevations below the summit, specifically Hermit Lake and Carroll, saw a near complete eradication of snowpack. On December 17th, Carroll reported 4.5 inches and Hermit Lake reported nearly 18 inches of snowpack, both of which were reduced to 0 by the morning of December 19th. The summit saw a similar pattern, with 5 inches of snow and ice reported at 4PM EST reduced to 1 inch by December 19th.

On December 15th, Tuckerman ravine reported up to 83 inches of snow on eastern aspects, with variable depths around the remainder of the bowl. This snowpack was characterized by a substantial layer of wind transported snow over multiple crusts with damp, granular snow underneath. This observed granular snow would suggest a general absence of ice beneath the ravine snowpack. By the next MWAC observation on December 21st, the snowpack was undermined by audibly running water and snowpack had been visibly reduced with bare rock newly visible around a majority of the ravine.

Ground Conditioning/Almanac Data:

The 2023 year was the 4th wettest on record at the NCON3 station, with a total of 61.7 inches liquid equivalent recorded by the end of December. December alone netted 7.35 inches liquid equivalent precipitation, 2.8 inches higher than average. However, the fall season preceding this event was cooler and drier than is typical, with only 10.44 inches liquid equivalent precipitation recorded for the September to November period, 3.16 inches below average. November alone saw 1.84 inches liquid equivalent precipitation less than average.

Stream Conditions:

This event's hydrologic response occurred shortly after the onset of steady rain and resulted in major flooding in the drainages surrounding Mount Washington. Gauge height measurements exceeded the threshold for major flooding at every gauge excepting that of the Amonoosuc River at Bethlehem which reached moderate levels. These flood heights were reached by midday on December 18th and had reduced back below the threshold for even minor flooding by December 19th. This response was intense, immediate, and relatively short lived.

This event produced the largest daily streamflow value (9810 ft3/s) ever recorded by the Saco River gauge in Bartlett, exceeding those of Hurricane Irene, Tropical Storm Philippe, and any other snowmelt event with the last decade. At the Ammonoosuc River at Bethlehem Gauge, this event (4760 ft3/s) ranks as the fourth largest recorded since 1939. The Saco River at Conway gauge has the longest record of the three, dating back to 1903, with the December 18, 2023 streamflow of 24300 ft3/s ranked sixth, exceeding that produced by Hurricanes Irene, Agnes, and Sandy. No larger out-of-season rain-on-snow event has ever been recorded at this gauge.

A log pearson function for the Ammonoosuc and Saco at Conway gauges yielded high recurrence intervals for both December 18th and 19th daily streamflow values. Streamflow at the Ammonoosuc gauge on the 18th produced an almost 800 year recurrence interval, followed by a 125 year recurrence interval for the 19th. The Conway gauge had similar results, 795 years for December 18th and 485 years for December 19th.

6) Discussion

A) Seasonality of ROS days

The work done in this study brought together temperature, snow metrics, and other meteorological variables recorded during four decades at Mount Washington, NH, from 1981-2020, which revealed a general seasonality of ROS days on the summit and a shortening winter season. Generally, the two most common times of the year for ROS days to occur at the summit in this study were early winter and early to mid-spring, and almost all ROS days occurred from October to May. Therefore, our results align well with a previous study by Mccabe et al. (2007) since they determined at the most common months for ROS are also from October to May. However, when comparing the two climatologies, it became apparent that there has been a shift in the seasonality of ROS days in recent years.

For the 1981-2010 climatology, the peak in early winter occurred in November with an average of around 4.5 ROS days per year. However, for the 1991-2020 climatology, the peak in early winter occurred in December with an average of 5.9 ROS days per month. The resulting increase in December was the largest out of any other month, with a value of 46%. However, the most ROS days occurred in April for both climatologies, with around 7-8 ROS days per month. However, the overall increase in ROS events during April across both climatologies was relatively small compared to the other months, and there wasn't a shift in the peak month like there was for the early winter peak. Therefore, this shift towards ROS days occurring later in the winter but during the same month in the spring indicates a shortening winter season.

This shift is also visually depicted in Figure #4 and aligns well with the results obtained by Murray et al. (2021). Temperatures at the summit in recent decades have warmed dramatically in the winter, with December having one of the highest warming rates compared to any other month, 0.22°C per decade (Murray et al. 2011). Additionally, during the past 15 years, the rate of warming at the summit has been faster than any 15-year period since 1935 and has begun to produce statistically significant long-term trends (Murray et al. 2011; Seidel et al. 2009). Therefore, the recent warming trends found by Murray et al. (2021) and the older warming trends found by Seidel et al. (2009) further explain why December experienced the largest increase in the average amount of ROS days relative to any other month across both climatologies analyzed in this study.

B) Weakening snow pact/delay in development of snow pact

The significant increase in ROS days in December across the two climatologies also supports the fact that the snowpack on the summit has weakened over the past few decades because of ROS days

occurring later in the year. The liquid precipitation types associated with ROS events tend to destabilize a snow pact due to their freeze-thaw cycles and overall snow melt (Il Jeong and Sushama 2018). Once a snowpack becomes destabilized by a ROS event, it often results in a weaker snowpack that can melt more easily (Singh et al. 1997a). Increasing ROS events in December also means that the summit can't start building its annual snow pack until later in the winter. Therefore, the snowpack on the summit is expected to weaken yearly as ROS days become increasingly prevalent in mid to late winter.

Additionally, other studies have previously observed trends in winter-thaw events at the summit and found increases in the duration and magnitude of said events when the dew point is warmer than 0°C, which is indicative of potential increases in snow-depth loss over time (Kelsey and Cinquino 2021). It is also further evidence of how ROS days have been increasingly weakening the snow pact over time since ROS days are often defined as having a temperature or dew point above 0°C and are frequently associated with winter thaw events (Tao et al. 2023; Würzer et al. 2016a).

Combining our results with the results of Kelsey and Cinquino (in press) reveals how ROS events at the summit have changed in recent years. Trends in ROS characteristics show that rapidly warming falls and winters in recent decades have resulted in more ROS events occurring later into winter than ever. Moreover, winter-thaw events with dew points greater than 0°C have been proven by Kelsey and Cinquino (press) to increase duration and magnitude in recent years at the summit. Therefore, the amount of ROS days occurring in mid to late winter has been increasing in recent years due to rapidly warming temperatures in December and winter-thaw events that have become longer and more powerful. So, storms that impacted the summit could stay as liquid precipitation instead of solid further into the winter and for a longer duration, which exacerbated the weakening of the snowpack.

C) Long term trends: Increasing number of ROS Days from 1981 to 2020

Predictions made by previous studies have stated how the frequency of ROS events will likely increase in high-elevation areas in the coming decades (Surfleet and Tullos 2013). Specifically, in a warmer future, areas around 2,000 and above in the Western US will see ROS days increase in frequency while the rest of the CONUS will mainly experience a decrease (Li et al. 2019). However, the results of this study have revealed that the summit has seen an increase in the frequency of ROS days in recent years despite being on the east coast. All slopes calculated by the Theil-Sen slope estimator and shown in figures #3 and #4 were positive for the annual amount of ROS days but had relatively weak coefficients of determinations. Furthermore, both climatologies passed the Mann-Kendall tests that were performed at the 5% significance level and the test at the 1% significance level, too.

With the summit being at an elevation of 1916m, it is almost at the expected elevation where ROS will increase in the west at 2000m (Li et al. 2019). Additionally, Li et al. (2019) discussed the regions of the CONUS with the highest historical frequency of ROS events, with the northeast being one of the primary four. Being near a large body of water, such as the Atlantic Ocean, tended to produce the highest frequencies of ROS events. In the northeast, warm, humid air from a body of water enables large snow accumulations in the winter and rainfall in the spring, resulting in the best conditions for large ROS events (Li et al. 2019). So, the summit is most likely experiencing an increasing frequency of ROS events due to the proximity to the Atlantic Ocean and its elevation above sea level, despite other studies concluding that the East Coast is more likely to see a decreasing frequency of ROS events (Li et al. 2019).

D) Case Study

While the December 2023 rain-on-snow event occurred too recently to be included in the climatology used by this paper, it serves as an example of the increasing magnitude of ROS events in the region. The December event resulted in the 6th highest runoff recorded by the Saco River gauge (Conway) since 1903. With the exception of Tropical Storm Philippe, the December event, lasting nearly 2 days, stands out as the shortest duration event to trigger daily runoff surpassing 21,000ft3/s at this stream gauge. Considering that the average duration of ROS events analyzed in this study is 1.7 days, it's noteworthy that an event fitting within this average ROS timeframe yielded runoff comparable to that of much longer events. These results are mirrored in the shorter records of the two other gauges located in more immediate subbasins. Of the larger recorded events, only two occurred without the influence of snowmelt, receiving 11.35 inches and 6.37 inches of liquid precipitation over four and two days, respectively, much higher totals than that of the December 2023 event. This is especially relevant given that the December snowpack was thinner than average at only 45cm and, regardless, rainfall has been found to be the more significant contributor to ROS runoff generation (Wayand et al. 2015). Each larger event saw either much higher precipitation totals or the addition of spring snowmelt, typically much deeper and denser than the early season snowpack of this 2023 event.

Relatively thin snowpack in December 2023 (as compared to that in the spring) in conjunction with the lack of ice within this snow created conditions favorable to a rapid runoff response, as seen in the stream gauge data (Singh et al. 1997b; Würzer et al. 2016b). Relatively thin snow cover also allowed for the near complete eradication of snowpack at all elevations on Mount Washington. It's likely that this snowmelt, particularly the near complete melting made possible by thin early season snowpack, allowed the 4.1in of liquid precipitation falling across 31 hours to result in a hydrologic forcing comparable to that caused by 6.37in of liquid precipitation falling across 32 hours during Tropical Storm Philippe. There exists space to examine why this event, falling on a thinner than average December snowpack, resulted in runoff values surpassing those of any other out of season rain on snow event in the region since 1903. As SWE, extent of snow-cover, and freeze/thaw elevations are named as primary driving forces behind ROS flooding, further investigation into these variables would be beneficial in developing a more thorough understanding of the development of this event(Rössler et al. 2013). Additionally, an examination of ground saturation, snowpack conditioning and the runoff generating potential of thin snowpacks would also increase understanding of this event. As upland basins are the most heavily influenced by ROS events (Freudiger et al. 2014b), an increase in frequency and magnitude of ROS events, as indicated by this study, have the potential to greatly impact Mount Washington and it's immediate subbasins. This event serves as a clear example of the high runoff and subsequent flooding potential resulting from increasing frequency and magnitude of out of season ROS events in the Mount Washington region.

7) Conclusions

Regarding climate change, the annual amount of precipitation that has fallen on the summit hasn't changed much over recent winters, but the proportion that has fallen as rain as opposed to snow has increased. Our study has shown an increasing trend in the number of ROS days experienced at the summit over recent decades. Therefore, the increasing number of ROS days shows how recent storms have been warming enough to transition snow to rain during winter. Furthermore, another trend found

by this study showed that the peak of ROS days in the early winter has been shifting later into the year. This further supports the idea that the proportion of precipitation that falls as rain, as opposed to snow, is increasing. It also reveals how the recent snow pact at the summit has become weaker in the early winter than in previous decades. With more ROS days occurring in December, the amount of melting among the summit's snowpack will increase.

As the work in our case study showed, a weaker and thinner snowpack earlier in the year can lead to potentially more impactful ROS events. This was further proven by a detailed analysis of the December 18-19, 2023, ROS event since it tended to be one of the most impactful flooding events in recorded history for various streams branching off from the summit. Over 31 hours, this event produced 4.1 inches of rainfall at the Mount Washington summit, almost completely eradicating snowpack at all elevations. The event caused significant flooding at most of the examined gauges, generating daily runoff numbers higher than any other non-spring ROS event in over a century. Calculated recurrence intervals for these discharge values reached nearly 800 years. As the frequency of these events increases in the region, ROS floods of this magnitude may become more common. Given the extent of damages caused by this event, the implications of the increased frequency of these floods could be significant for those communities and ecosystems on and below Mount Washington. Furthermore, the characteristics of the December 18-19, 2023 ROS event also aligned very well with the attributes of ROS events found in this study.

In conclusion, the results show the importance of understanding the characteristics and long-term trends of ROS events at the summit of Mount Washington. Other than tropical storms, ROS events have resulted in some of the most severe flooding events around Mount Washington. With more ROS days expected to occur, gaining a better understanding of how to forecast them and best prepare for them will be crucial for mitigating their impacts. Therefore, there is still a need to understand the weather patterns that commonly cause ROS events to be better prepared for them. Further work examining the factors contributing to the historic runoff of the December 2023 ROS event would greatly benefit from understanding ROS flooding in the Northeast.

Bibliography

Brown, P. J., R. S. Bradley, and F. T. Keimig, 2010: Changes in extreme climate indices for the Northeastern United States, 1870-2005. *J Clim*, **23**, 6555–6572, https://doi.org/10.1175/2010JCLI3363.1.

Dethier, D. P., N. Williams, and J. F. Fields, 2022: Snowmelt-Driven Seasonal Infiltration and Flow in the Upper Critical Zone, Niwot Ridge (Colorado), USA. *Water (Switzerland)*, **14**, https://doi.org/10.3390/w14152317.

Freudiger, D., I. Kohn, K. Stahl, and M. Weiler, 2014a: Large-scale analysis of changing frequencies of rain-on-snow events with flood-generation potential. *Hydrol Earth Syst Sci*, **18**, 2695–2709, https://doi.org/10.5194/hess-18-2695-2014.

——, ——, ——, and ——, 2014b: Large-scale analysis of changing frequencies of rain-on-snow events with flood-generation potential. *Hydrol Earth Syst Sci*, **18**, 2695–2709, https://doi.org/10.5194/hess-18-2695-2014.

Graham, R. M., L. Cohen, A. A. Petty, L. N. Boisvert, A. Rinke, S. R. Hudson, M. Nicolaus, and M. A. Granskog, 2017: Increasing frequency and duration of Arctic winter warming events. *Geophys Res Lett*, **44**, 6974–6983, https://doi.org/10.1002/2017GL073395.

Hans-O, P., 2023: Summary for Policymakers. *Climate Change 2022 – Impacts, Adaptation and Vulnerability*, Cambridge University Press, 3–34.

Heath, R. C., North Carolina. Department of Natural Resources and Community Development., and Geological Survey (U.S.), 2004: *Basic ground-water hydrology*. U.S. Geological Survey, 86 pp.

Il Jeong, D., and L. Sushama, 2018: Rain-on-snow events over North America based on two Canadian regional climate models. *Clim Dyn*, **50**, 303–316, https://doi.org/10.1007/s00382-017-3609-x.

Kelsey, E. P., and E. Cinquino, 2021: The climatological rise in winter temperature-and dewpoint-based thaw events and their impact on snow depth on mount washington, new hampshire. *J Appl Meteorol Climatol*, **60**, 1361–1370, https://doi.org/10.1175/JAMC-D-20-0254.1.

Kimball, K. D., and D. M. Weihrauch, 2000: *Alpine Vegetation Communities and the Alpine-Treeline Ecotone Boundary in New England as Biomonitors for Climate Change*.

Kotlarski, S., and Coauthors, 2014: Regional climate modeling on European scales: a joint standard evaluation of the EURO-CORDEX RCM ensemble. *Geosci Model Dev*, **7**, 1297–1333, https://doi.org/10.5194/gmd-7-1297-2014.

Leak, W. E., and R. E. Graber, *Forest Vegetation Related to Elevation in The White Mountains of New Hampshire*.

Li, D., D. P. Lettenmaier, S. A. Margulis, and K. Andreadis, 2019: The Role of Rain-on-Snow in Flooding Over the Conterminous United States. *Water Resour Res*, **55**, 8492–8513, https://doi.org/10.1029/2019WR024950.

Mann, H. B., 1945: Nonparametric Tests Against Trend. *Econometrica*, **13**, 245.

Mccabe, G. J., M. P. Clark, and L. E. Hay, 2007: Rain-on-Snow Events in the Western United States. *Bull Am Meteorol Soc*, **88**, 319–328, https://doi.org/10.1175/BAMS-88-3-3I9.

Murray, G. L. D., and Coauthors, 2011: *Northeastern Naturalist Climate Trends on the Highest Peak of the Northeast: Mount Washington, NH*. 64–82 pp.

——, and Coauthors, 2021: *Northeastern Naturalist Climate Trends on the Highest Peak of the Northeast: Mount Washington, NH*. 64–82 pp.

National Weather Service, 1998: *Training Guide in Surface Weather Observations*.

Pall, P., L. M. Tallaksen, and F. Stordal, 2019: A Climatology of Rain-on-Snow Events for Norway. *J Clim*, 6995–7016, https://doi.org/10.1175/JCLI-D-18.

Peeters, B., and Coauthors, 2019: Spatiotemporal patterns of rain-on-snow and basal ice in high Arctic Svalbard: detection of a climate-cryosphere regime shift. *Environmental Research Letters*, **14**, 015002, https://doi.org/10.1088/1748-9326/aaefb3.

Poschlod, B., Ø. Hodnebrog, R. R. Wood, K. Alterskjaer, R. Ludwig, G. Myhre, and A. J. Sillmann, 2018: Comparison and Evaluation of Statistical Rainfall Disaggregation and High-Resolution Dynamical Downscaling over Complex Terrain. *J Hydrometeorol*, **19**, 1973–1982, https://doi.org/10.1175/JHM-D-18.

Rennert, K. J., G. Roe, J. Putkonen, and C. M. Bitz, 2009: Soil thermal and ecological impacts of rain on snow events in the circumpolar arctic. *J Clim*, **22**, 2302–2315, https://doi.org/10.1175/2008JCLI2117.1.

Rössler, O., P. Froidevaux, U. Börst, R. Rickli, O. Martius, and R. Weingartner, 2013: A non-forecasted rain-on-snow flood in the Alps Retrospective analysis of a non-forecasted rain-on-snow flood in the Alps-a matter of model-limitations or unpredictable nature? A non-forecasted rain-on-snow flood in the Alps A non-forecasted rain-on-snow flood in the Alps. *Hydrol. Earth Syst. Sci. Discuss*, **10**, 12861–12904, https://doi.org/10.5194/hessd-10-12861-2013.

Seidel, T., D. Weihrauch, K. Kimball, A. Pszenny, R. Soboleski, E. Crete, and G. Murray, 2009: Evidence of climate change declines with elevation based on temperature and snow records from 1930s to 2006 on Mount Washington, New Hampshire, U.S.A. *Arct Antarct Alp Res*, **41**, 362–372, https://doi.org/10.1657/1938-4246-41.3.362.

Seidel, T. M., A. N. Grant, A. A. P. Pszenny, and D. J. Allman, 2007: Dewpoint and humidity measurements and trends at the summit of Mount Washington, New Hampshire, 1935-2004. *J Clim*, **20**, 5629–5641, https://doi.org/10.1175/2007JCLI1604.1.

Sen, P. K., 1968: Estimates of the Regression Coefficient Based on Kendall's Tau. *J Am Stat Assoc*, **63**, 1379–1389, https://doi.org/10.1080/01621459.1968.10480934.

Singh, P., G. Spitzbart, H. Hübl, and H. W. Weinmeister, 1997a: *Hydrological response of snowpack under rain-on-snow events: a field study*. 1–20 pp.

Singh, P., G. Spitzbart, H. Hübl, and H. W. Weinmeister, 1997b: Hydrological response of snowpack under rain-on-snow events: A field study. *J Hydrol (Amst)*, **202**, 1–20, https://doi.org/10.1016/S0022-1694(97)00004-8.

Sobota, I., P. Weckwerth, and T. Grajewski, 2020: Rain-On-Snow (ROS) events and their relations to snowpack and ice layer changes on small glaciers in Svalbard, the high Arctic. *J Hydrol (Amst)*, **590**, 125279, https://doi.org/https://doi.org/10.1016/j.jhydrol.2020.125279.

Surfleet, C. G., and D. Tullos, 2013: Variability in effect of climate change on rain-on-snow peak flow events in a temperate climate. *J Hydrol (Amst)*, **479**, 24–34, https://doi.org/https://doi.org/10.1016/j.jhydrol.2012.11.021.

Tao, J., X. Cheng, L. Zheng, X. X. Xiao, X. Y. Zhong, Q. Liang, Z. Q. Zhang, and H. Lin, 2023: Performance of climate reanalyses in the determination of pan-Arctic terrestrial rain-on-snow events. *Advances in Climate Change Research*, **14**, 522–536, https://doi.org/10.1016/j.accre.2023.08.002.

Theil, H., 1950: *A Rank-Invariant Method of Linear and Polynomial Regression Analysis I.*

Vickers, H., P. A. Mooney, E. Malnes, and H. Lee, 2022: Comparing rain-on-snow representation across different observational methods and a regional climate model. *The Cryosphere Discuss*, https://doi.org/10.5194/tc-2022-57.

Vikhamar-Schuler, D., K. Isaksen, J. E. Haugen, H. Tømmervik, B. Luks, T. V. Schuler, and J. W. Bjerke, 2016: Changes in Winter Warming Events in the Nordic Arctic Region. *J Clim*, **29**, 6223–6244, https://doi.org/10.1175/JCLI-D-15-0763.1.

Wayand, N. E., J. D. Lundquist, and M. P. Clark, 2015: Modeling the influence of hypsometry, vegetation, and storm energy on snowmelt contributions to basins during rain-on-snow floods. *Water Resour Res*, **51**, 8551–8569, https://doi.org/10.1002/2014WR016576.

Würzer, S., T. Jonas, N. Wever, and M. Lehning, 2016a: Influence of initial snowpack properties on runoffformation during rain-on-snow events. *J Hydrometeorol*, **17**, 1801–1815, https://doi.org/10.1175/JHM-D-15-0181.1.

——, ——, ——, and ——, 2016b: Influence of initial snowpack properties on runoffformation during rain-on-snow events. *J Hydrometeorol*, **17**, 1801–1815, https://doi.org/10.1175/JHM-D-15-0181.1.

Young, S., and J. Young, 2021: Overall Warming with Reduced Seasonality: Temperature Change in New England, USA, 1900–2020. *Climate*, **9**, 176, https://doi.org/10.3390/cli9120176.

Yue, S., and P. Pilon, 2004: A comparison of the power of the t test, Mann-Kendall and bootstrap tests for trend detection. *Hydrological Sciences Journal*, **49**, 21–37, https://doi.org/10.1623/hysj.49.1.21.53996.

surficialmapwashingtonkey.